

Water/oil emulsion and asphaltene instability in different formations during low-salinity waterflooding: an experimental study

Amirhossein Salari, Ali Balavi, Shahab Ayatollahi*, Hassan Mahani*

Department of Chemical and Petroleum Engineering, Sharif University of Technology, Tehran, Iran, postal code: 145888694

*Corresponding authors' Email and mobile numbers (Shahab Ayatollahi, shahab@sharif.edu, +9891711847; Hassan Mahani, hmahani@sharif.edu, +98913362042)

Abstract

Previous studies have extensively investigated the effects of salinity on asphaltene behavior at the water-oil contact surface during Low-salinity waterflooding. However, the influence of rocks has often been overlooked. This study investigates the impact of rock type (calcite/quartz) on these phenomena in the presence of various brines (Formation Water (FW), Sea Water (SW), 2 and 10 times diluted SW (2DSW, 10DSW), Distilled Water (DW)). UV-Vis spectroscopy was used to assess the asphaltene separation from fresh or aged bulk oil with brine, by using the "indirect method". Microscopic analysis of water droplet size was performed to evaluate emulsion stability. The results demonstrate that the UV-Vis absorbance for fresh oil is approximately 13.6 and that decreases to 11, 10.5, and 10.5 for the 2DSW/oil, calcite/SW/oil, and quartz/2DSW/oil emulsions, respectively. Additionally, the results show that for rock/FW/oil emulsion, compared to quartz, calcite presence increases asphaltene precipitation/deposition by about 38 wt.%. Furthermore, the findings reveal that, across all salinities, the average size of water droplets is larger when calcite is present than quartz, suggesting greater instability in the calcite. These outcomes align with the results of Interfacial tension (IFT) measurement, FTIR spectral analysis of oil, and zeta-potential determination for suspended calcite/quartz particles in different brines.

Keywords: Asphaltene instability, Emulsion formation, Low-salinity Waterflooding, UV-Vis spectroscopy, Carbonate rocks, Sandstone rocks

1. Introduction

Low-salinity waterflooding (LSWF) is a promising method for improving oil recovery in oil reservoirs with low recovery rates. Although a definitive recovery mechanism remains uncertain, empirical evidence suggests that adjusting ion type and concentration in the water phase can enhance oil recovery by altering reservoir and fluid properties such as wettability, permeability, capillary pressure, and interfacial properties between water and oil [1-8].

Research suggests that LSWF primarily is an interfacial phenomenon; and asphaltenes, identified as the most significant polar component in the oil phase, are crucial in these interfacial interactions. They can either gather at the water/oil interface or directly adsorb onto the rock surface [6, 9, 10]. The affinity of asphaltenes to the oil/brine interface and the subsequent

formation of undesirable emulsions can result in oil entrapment, ultimately diminishing the overall potential for oil recovery [11]. Moreover, the deposition of asphaltenes on the surface of reservoir rocks may cause damage to the reservoir formation [9, 12-16]. It is noteworthy that in certain instances, asphaltene deposition and emulsion formation can contribute to enhanced oil recovery(EOR) by augmenting sweeping efficiency.

The role of asphaltenes during waterflooding has been extensively studied by various researchers, and the existing studies can be categorized into two groups: fluid/fluid interaction and rock/fluid interaction. These groups are discussed in the following paragraphs.

Asphaltene particles have polar and non-polar parts in their structure. Therefore, focusing on their fluid-fluid interface, the polar part interacts with the available ions in the brine and causes asphaltenes to be attracted to the brine/oil interface. The accumulation of asphaltene particles on the interface causes them to act as natural surfactants [17, 18]. This accumulation creates a viscoelastic interfacial layer around water droplets, impacting critical parameters such as emulsion stability, interfacial tension (IFT), and water droplet size [19]. The role of asphaltenes in this process depends on factors such as their concentration in the oil phase, the onset points of asphaltene precipitation, and the pH and salinity of the aqueous phase (including the type and concentration of ions in the aqueous phase) [9, 20-22].

Various approaches have been used to assess asphaltene stability in water-in-oil emulsion, such as analyzing brine/oil phase properties or examining properties of the water/oil interface such as viscoelasticity and IFT. Studies have shown that higher brine salinity enhances asphaltene stability, with divalent cations having a stronger effect than monovalent cations [17, 18, 23, 24]. Decreasing brine salinity leads to more stable emulsions and lower IFT, while increased salinity

results in greater asphaltene aggregation. Overall, asphaltene behavior at the interface is influenced by factors such as brine salinity, asphaltene concentration, and ionic strength [25-27].

All of these studies have been performed in non-porous media, disregarding the influence of rock presence on asphaltene behavior. However, it is known that asphaltene adsorption onto rock surfaces during waterflooding significantly affects reservoir rock wettability [28, 29]. Experimental evidence suggests that asphaltene adsorption on rocks depends on various parameters including asphaltene concentration, rock type, flow rate, and brine characteristics (salinity, pH, etc.) [30-33]. Researchers have employed different methods such as Quartz Crystal Microbalance (QCM) to investigate asphaltene deposition on solid surfaces such as silica [25, 26]. Meanwhile, others have utilized natural or artificial porous media, such as core samples or rock packs, to assess asphaltene deposition [9, 12, 15, 16, 34, 35]. The presence of rock can also influence emulsion stability by promoting Pickering emulsion formation. The stability of Pickering emulsions depends on several parameters, including the type of emulsion (water-in-oil or oil-in-water) [36-38].

Our recent studies indicate that the presence of calcite rock affects asphaltene behavior, prompting further investigation on the impact of different rock types on asphaltene instability during LSWF [39]. This comprehensive approach aims to understand factors influencing asphaltene deposition, crucial because unstable asphaltene can lead to pore plugging and formation damage.

To investigate asphaltene performance and its impact on emulsion stability, we followed the modified indirect method outlined by Balavi et al. [39]. This involved measuring the UV-Vis absorbance of the oil phase before and after contact with the aqueous phase and evaluating water droplet size distribution. Additionally, we measured the interfacial tension (IFT) between the

fresh or aged oil phase and different brines, assessed the zeta-potential of suspended calcite or quartz particles in various brines, and conducted Fourier Transform Infrared (FTIR) analysis of the oil phase to interpret and understand the results. The experimental procedures and the outcomes are elaborated upon in the subsequent sections.

2. Materials and Methods

The conducted experiments in this study involve static tests using a particular crude oil sample, and various target brines for EOR purpose. Two types of solid particles (mainly composed of quartz and calcite minerals) were selected to represent end-members of sandstone and carbonate formations respectively. Analytical tests including FTIR, zeta-potential measurement, UV-Vis spectroscopy, IFT determination, and emulsion stability evaluation were conducted to assess the properties of the liquid and solid phases and their interactions, and to interpret the results of static tests on asphaltene instability.

2.1. Crude Oil sample

A crude oil sample obtained from an oil reservoir in southwestern Iran, known for asphaltene deposition issues, underwent purification before experiments. The purification involved removing dissolved gas, suspended solids, and water droplets through simultaneous evacuation and filtration. Asphaltene isolation followed the IP-143 standard test method, involving mixing the oil sample with normal pentane, filtration, and reflux heating with pentane and toluene [40]. The weight fraction of asphaltene was determined from the remaining sediment. The key properties of the oil sample are outlined in Table 1.

The oil sample used in the study has a total acid number (TAN) exceeding 0.5 mg KOH/g oil, categorizing it as acidic oil with a prevalence of carboxylic groups over amine groups. Consequently, the oil/brine interface is expected to be negatively charged.

2.2. Brines

To prepare the target brine samples, including formation water (FW), seawater (SW), 2-times diluted seawater (2DSW), 10-times diluted seawater (10DSW), and distilled water (DW), specific amounts of salts such as NaCl, KCl, CaCl₂·2H₂O, MgCl₂·6H₂O, Na₂SO₄, and NaHCO₃ were dissolved in distilled water. These salts, sourced from Dr. Mojallali Company, were of laboratory-grade quality, with a purity exceeding 99%. Table 2 outlines the concentrations of these salts used in preparing different brines.

2.3. Other Chemicals

For this investigation, laboratory-grade normal pentane (n-C₅) and toluene, with a purity exceeding 99%, were obtained from Shimibio Company, Iran. These solvents were used for the extraction of asphaltenes and for diluting the supernatant fluid (oil) before UV-Vis absorbance measurement is taken.

2.4. Rock Characteristics (Sandstone and Calcite particles)

In this study, high-purity sandstone containing 98.5% quartz and 1.5% calcite, along with calcite rocks, were crushed to produce pulverized material. Sieves with a micron size ranging from 75 to 150 were used to ensure uniformity in the size of rock particles across all experiments. Particles

within this size range were utilized in the experimental setups to maintain consistency. The XRD spectrum of the sandstone sample is provided in the **Supplementary Material, Appendix A, Figure S.1.**

2.5. FTIR analysis of oil

A PerkinElmer ATR-FTIR spectrometer was employed to conduct the FTIR analysis of oil samples, utilizing a resolution of 1 cm^{-1} , spanning the spectral range from 400 to 4000 cm^{-1} . These tests were conducted to identify the functional groups present in the oil.

2.6. Zeta-potential measurement

The zeta-potential of suspended calcite/quartz particles in various brine solutions was determined using a Zetasizer Nano instrument from Malvern. Following the methodology outlined by Saraji et al. and Mahani et al., calcite/quartz particles with a size ranging from 75 to $150\text{ }\mu\text{m}$ were introduced into 25 cc of each brine sample. The mixture underwent sonication for 30 minutes to achieve homogenization and was then allowed to rest for an hour to reach equilibrium conditions before conducting zeta-potential measurements [35, 41]. Each test was repeated three times to determine the average value and the standard deviation of the measured value.

The impact of particle size on effective zeta-potential is significant, with smaller particles being more influenced by fluid flow and interactions with other particles, resulting in a higher absolute value of effective zeta-potential compared to larger particles [36]. However, in this study, rock particles within a specific and consistent size range of 75 - $150\text{ }\mu\text{m}$ were used for both sandstone and calcite. Additionally, zeta-potential was measured after the brine/rock mixture reached

equilibrium, without considering variations in particle size during the research, thus ensuring that it did not influence the obtained results.

2.7. UV-Vis absorbance measurement

In this research, a T80+ UV/Vis spectrometer (Ultraviolet–visible spectrometer) from PG Instruments Ltd. was employed to quantify the UV-Vis absorbance of the supernatant fluid following the centrifugation process. Air was utilized as a blank sample for this purpose.

2.8. Oil-brine IFT measurement

In this study, the interfacial tension (IFT), a crucial interfacial characteristic, was measured for each fresh or aged oil with various brines using the pendant drop method. Throughout the study, the IFT between fresh oil and different brines is referred to as the initial IFT, while the IFT between aged oil (i.e., oil that has come into contact with brine during the emulsion phase and subsequently separated during centrifugation) and various brines is denoted as the final IFT.

In the experiments involving rock particles or presence, a specific quantity of rock material (calcite/quartz) was mixed with different brines and allowed to age for 24 hours. Then the mixture underwent filtration using Chemlab cellulose filter paper with a pore diameter of 125 micrometers, along with a metal mesh with a micron size of 37 placed on top of each other to prevent tearing of the filter paper and hinder the passage of rock particles. The filtered brines were used for initial and final IFT measurements.

As the composition of the brine remains constant for each experiment set and both initial and final IFT measurements were conducted under ambient conditions, any observed changes in their

values depends on the properties of the oil phase. According to existing literature, the separation of heavy oil fractions, such as asphaltenes, during the centrifugation step is the primary factor contributing to alterations in IFT [17, 18, 42].

2.9. Emulsion Stability

In the context of LSWF, the interaction between oil and water directly influences emulsion formation and stability. This study investigates emulsion stability to understand the behavior of the water/oil interface. Empirical evidence suggests that in a water-in-oil emulsion system, emulsion stability decreases as the size of water droplets increases [37, 38, 43].

To analyze the distribution of water droplet sizes, the optical microscopy method was employed in this study [44-46]. Small samples were extracted from the emulsion phase using a syringe at two different time intervals: 1 hour and 24 hours into the emulsification process. Sampling was conducted while continuously stirring the emulsion to ensure representativeness throughout the mixture. These samples were carefully placed on a microscope glass slide and observed using high-resolution digital microscopy with a Dino Light microscope (at 1000x magnification). Image processing with ImageJ® software was used to determine the distribution of water droplet sizes. Each test was repeated at least three times, and the average value was reported as the final result.

2.10. Design of experiments

In our previous study, we demonstrated the significant effect of calcite on oil/brine interaction and asphaltene precipitation [39]. In this study, we delve into the impact of rock type on this

phenomenon. Initially, we investigate how water salinity affects asphaltene stability. Subsequently, we examine the influence of different grain types (calcite and quartz) on both asphaltene and emulsion stability.

Given that we only explored the effects of rock type and salinity in this study, a factorial experimental design approach was not necessary. However, for future studies where the number of variables and their levels are more extensive, we plan to employ experimental design and statistical approaches to streamline the experimentation process. The experimental procedures for these investigations are described in the following section in detail.

2.10.1. Investigation of the effect of brine types on asphaltene stability

In this study, we evaluate asphaltene stability within an emulsified system using an indirect method. Initially, 60 cc of oil was slowly poured into a beaker containing 40 cc of brine and stirred at 1000 rpm for 24 hours using an Alfa D-500 stirrer from Shimibio Company. At 1 and 24 hours into the emulsification process, two small samples were collected to assess emulsion stability.

Following emulsification, samples underwent centrifugation for 12 minutes at a speed of 10,000 revolutions per minute (equivalent to 9168 times the gravity acceleration). This process separated water droplets and suspended asphaltene particles from the mixture, resulting in two distinct phases: the upper oil phase and the lower water phase.

The upper or supernatant phase, which was opaque, was unsuitable for UV-Vis spectroscopy. Therefore, it was diluted with toluene at a 1:4 volume ratio, and UV-Vis spectroscopy was conducted at a wavelength of 800 nm, where the absorbance for toluene is nearly zero. Results

were corrected to eliminate the influence of toluene that was added as a diluting agent, as detailed in our previous work [39].

The experimental procedure is illustrated in Figure 1. All experiments were conducted under ambient pressure and temperature conditions and repeated 2-3 times to ensure reproducibility of the results.

2.10.2. Investigation of the effect of different rock (calcite/quartz) presence on asphaltene and emulsion stability

To investigate the impact of rock presence on asphaltene and emulsion stability, two common types of reservoir rock (calcite representing carbonate and quartz representing sandstone) were selected. Calcite/silica particles were introduced into various brine samples at a ratio of 0.1 gr/cc and aged for 24 hours. Subsequently, different emulsions were prepared by gradually adding 40 cc of brine/rock mixture to 60 cc of an oil sample while stirring at 1000 rpm. To ensure homogeneity, the oil/brine/rock mixture was stirred for 24 hours.

After the aging period, the mixture was allowed to settle and then filtered using a filter paper with a pore diameter of 125 micrometers along with a metal mesh with a micron size of 37 to separate the rock particles from the liquid phases (brine and oil), with the assistance of a vacuum pump. This process took approximately 30 minutes and led to emulsion instability. To address this, the filtered emulsion was stirred once more at 1000 rpm for 1 hour and subsequently analyzed following the same procedure as outlined earlier.

In this case, there are two potential sites for asphaltene adsorption: the water/oil interface and the rock surface. The solid component consisted of rock particles, adsorbed asphaltenes on the rock surface, loosely bound and suspended asphaltenes, trapped oil, and brine between the rock

particles. To remove any suspended asphaltene and trapped oil, the solids underwent a solvent-washing process with n-C5. It was then washed with distilled water to dissolve and remove any precipitated ions and trapped brine. The remaining sediment mixture was subsequently heated to 80°C for 24 hours to vaporize any remaining water and light hydrocarbons and to dry the sediment. In this step, the remaining sediment mixture comprised of rock and asphaltenes adsorbed onto the rock surface.

To quantify the amount of adsorbed asphaltenes, the sediment was washed with toluene to extract the adsorbed asphaltenes. Finally, the UV-Vis absorbance of the filtered toluene (containing the extracted asphaltenes) was measured. Asphaltene content can be calculated using a calibration curve, as described in the previous work and other papers [15, 39, 47].

3. Results and discussion

In the following sections, we present and discuss the experimental results of asphaltene instability in various brines and the effect of rock type on this behavior.

3.1. Asphaltenes deposition

The published studies have found that higher asphaltene content in a hydrocarbon solution correlates with greater UV-Vis absorbance [16, 28, 48]. To assess asphaltene migration from the oil phase to the water/oil interfaces or rock surfaces, UV-Vis absorbance of the aged oil after centrifugation was measured. Results show consistently lower absorbance in all emulsified systems compared to fresh oil, indicating asphaltene migration prompted by brine and rock presence. Rock presence leads to a more significant reduction in absorbance, suggesting greater

asphaltene migration. Emulsions with calcite particles show higher absorbance at lower salinities, but this trend reversed at higher salinities. Further explanation will be provided in subsequent sections.

3.1.1. Test Results Without Rock

In emulsified systems without rock presence, asphaltene stability varies notably with different brine types. Formation water (FW) yields the highest stability, whereas two times diluted seawater (2DSW) leads to more asphaltene leaving the bulk oil. Overall, asphaltene stability shows a non-monotonic trend relative to salinity: FW > DW > 10DSW > SW > 2DSW. This behavior stems from the "salt in/salt out effect". At low salinities, such as in 2DSW, "salt in" causes asphaltene to adsorb onto the water-oil interface; as salt concentration rises, "salt out" prevails, enhancing stability. This aligns with other researchers' findings. The impact of high salinity is debatable; Stability of asphaltene in contact with FW surpasses other brines but remains lower than that in fresh oil, contrary to prior high-salinity studies. Notably, this study uses a FW containing different types of salts, unlike the prior single-salt brine studies [5, 18, 20, 42].

The other reason is that at high salinity divalent ions such as Ca^{+2} and Mg^{+2} disrupt hydrogen bonds between water molecules in the brine phase and polar components in the oil phase. Consequently, UV-Vis absorbance increases when salinity changes from approximately 24,000 to 190,000 ppm (from 2DSW to FW), as depicted in Figure 2. Mokhtari et al. suggest that at high salt concentrations, divalent ions act as nuclei around which asphaltene molecules aggregate. Shojaati et al. propose that, according to the "chelation" theory, asphaltene adsorption to the water/oil interface is primarily due to the asphaltene-ion bond in the presence of divalent ions.

Their results indicate that divalent cations have a more significant impact on asphaltene instability, and among ions with the same electrical charge, smaller ones play a more critical role in asphaltene stability [18, 20].

3.1.2. Test Results with Rock Presence

It is worth noting that parameters, such as pH and ionic strength, influence the stability of the brine film. In summary, the stability of thin films (thinner than 100 nm) depends on the surface forces, including electrostatic, Van der Waals, and structural forces, acting between two interfaces. Electrostatic forces are influenced by the ions present and the surface charge of the oil and rock surfaces, and they can be either attractive or repulsive. Van Der Waals forces are relatively weak attractive forces between the oil and rock surfaces.

Electrostatic forces between calcite/quartz and asphaltene were examined. Our experimental results show rock presence impacts asphaltene performance in two ways: i) rock dissolution alters brine properties such as pH, affecting asphaltene absorption at the water/oil interface; ii) rock presence provides new deposition sites for asphaltenes. These aspects are further discussed in the following section.

3.1.2.1. pH change due to mineral dissolution

Geochemical studies have revealed that the interactions between calcite/quartz and brine can result in changes in certain brine properties, notably the pH. These variations in pH have a significant impact on the behavior of the asphaltene molecules at the water/oil interface [30, 31,

49-51]. Fig. 3 illustrates the pH differences resulting from the dissolution of rock for various brines.

Figure 3 depicts rock dissolution in all brines, correlating with increased pH values. This pH rise is more pronounced at lower salinity and initial pH values, consistent with previous findings. Research indicates pH changes notably affect interfacial properties such as IFT and emulsion stability. Higher pH leads to increased asphaltene adsorption at the water/oil interface, resulting in a more stable emulsion [21, 22, 34, 52]. In this study, the pH increase resulted in more asphaltene separation during centrifugation, consequently reducing UV-Vis absorbance.

3.1.2.2. Rock surface electrical charge in different brines

To comprehend the deposition of asphaltenes on the rock surface, it is essential to scrutinize the forces between the oil (asphaltenes) and the rock surface. Investigating this phenomenon entails analyzing the surface electrical charge of both the rock and the crude oil. In this regard, the zeta-potential of suspended rock particles (including calcite and quartz particles) in various brines was measured, and the findings are illustrated in Figure 4.

As illustrated in Figure 4, the zeta-potential of both calcite and quartz particles shows a significant dependency on the type of brine. At lower salinities, the zeta-potential tends to be more negative, shifting towards a more positive value as salinity increases. These observations corroborate findings from previous studies [21, 22, 34, 35]. Additionally, the results suggest that quartz particles possess a more negatively charged surface compared to calcite particles.

3.1.2.3. FTIR results for bulk oil

On a related note, as previously mentioned in sections 2.1 and 2.4, the oil phase in this study has a TAN of approximately 0.11 mg KOH/g oil, classifying it as acidic oil with a negative electrical surface charge. Additionally, FTIR tests with a resolution of 1 cm^{-1} in the range of $400\text{--}4000\text{ cm}^{-1}$ were conducted to identify the functional groups present in the fresh oil. The FTIR absorbance results are presented in Figure 5.

As illustrated in Figure 5, the peaks in the FTIR analysis indicate that the crude oil contains a higher concentration of carboxylic groups compared to amine groups. Consequently, both the TAN and FTIR results suggest that the electrical surface charge of the oil phase, and consequently the asphaltene particles, can be characterized as negative.

3.1.2.4. Asphaltene Adsorption

Based on the zeta-potential results for rock-brine and the FTIR results it can be concluded that, at low salinities, when both asphaltene particles and calcite/quartz surfaces carry a negative charge, repulsive forces exist between the two interfaces (oil/brine and rock). With an increase in ion concentration, the zeta-potential for both calcite and quartz particles shifts to a more positive value, resulting in a reduction of repulsive forces. This decrease in stability of the existing film around the rock particles leads to greater asphaltene adsorption. Similar findings have been reported by other researchers [34, 53].

Figure 6 illustrates asphaltene deposition quantities on the rock surface. Comparatively, more asphaltene adsorption is noted on calcite particles than on quartz particles in the emulsion samples. Given quartz particles' more negative surface electrical charge than calcite particles, it

suggests weaker attractive forces between asphaltenes and quartz compared to calcite. Additionally, results indicate electrostatic forces are influenced by brine ion concentration and type, beside rock type. It is crucial to recognize that asphaltene deposition on calcite/quartz surfaces increases the covered rock surface area. However, since the surface area increase is limited, it is not the primary factor governing increased adsorption [34].

3.2. IFT and Emulsion stability (droplet size determination) results

3.2.1. IFT Results

As discussed earlier, asphaltene adsorption onto the water/oil interface plays a crucial role in influencing interfacial characteristics, including IFT and emulsion stability. To validate the UV-Vis results, this study measured the IFT between fresh/aged oil and various brines. The results of initial and final IFT measurements are illustrated in Figures 7 and 8, respectively.

Figure 7 demonstrates that at low salinity, the salt-in effect attracts asphaltenes to the water/oil interface due to brine ions, leading to an initial IFT decrease. However, at moderate to high salinity levels, the salt-out effect prevails, causing a reversal in the IFT change trend. Consequently, the IFT change versus salinity exhibits a non-monotonic pattern, with the lowest IFT occurring in SW/oil emulsion systems for both no-rock and rock presence experiments. Moreover, dissolution of rock particles (calcite/quartz) in all brines decreases IFT, with greater change observed for calcite compared to quartz. As discussed in Section 3.1.2.1, rock dissolution increases pH, leading to an IFT decrease, aligning with the findings in the literature [21, 22, 34, 35, 54].

The results depicted in Figures 7 and 8 indicate that, across all scenarios, the final IFT is consistently higher than the initial IFT. This discrepancy is attributed to changes in the composition of the oil phase, as the same brine sample is used for measuring both initial and final IFT in this study. The centrifugation process, which separates asphaltenes, leads to an increase in the final IFT.

For a more comprehensive analysis of rock/brine/oil interaction, the change in UV-Vis absorbance (based on a fresh oil sample) versus the change in IFT (representing the difference between initial and final IFT) is depicted in Figure 9.

The study highlights that both UV-Vis absorbance and IFT show a non-monotonic relationship with salinity, as depicted in Figure 9. The extremum points for changes in IFT and UV-Vis absorbance don't align consistently across different experiments using the same brine. Notably, the maximum change in IFT is observed when using 10DSW brine across various scenarios, except those involving rock, calcite, or quartz. For experiments without rock and those with quartz, the highest UV-Vis absorbance occurs with emulsions created using 2DSW, while for calcite experiments, it happens with SW solutions.

The introduction of rock particles into emulsified systems causes further separation of asphaltene particles from the oil, as they adhere to the rock surface. The attraction force between the rock surface and asphaltene particles is stronger for calcite compared to quartz, especially in higher salinity brines. Consequently, in calcite experiments, the change in UV-Vis absorbance is greater than the change in IFT at higher salinities.

3.2.2. Emulsion stability (droplet size determination)

In Section 2.8, numerous micrographs were taken at 1 and 24 hours during emulsion preparation and analyzed with ImageJ® software. The images clearly show the formation of water-in-oil emulsions, where aqueous phase droplets are dispersed in oil. Only water droplet sizes were measured and statistically evaluated. Figures 10 and 11 depict the mean water droplet sizes in various brine/oil emulsion systems, while Table 3 provides the number of water droplets within specific areas for each case. The microscopic images of water-in-oil emulsions with each brine can be found in the **Supplementary Material, Appendix B, Figures S.2 through S.8**.

The analysis of Figures 10 and 11 reveals no significant change in the mean size of water droplets after 1 and 24 hours of emulsion preparation, indicating a stable asphaltene content at the water/oil interface within the initial hour. Furthermore, the data illustrates that increasing salinity decreases water droplet size, reaching its minimum in SW/oil emulsions before reversing. This trend aligns with changes observed in the initial IFT. Although there is no universal mathematical correlation linking water droplet size to IFT, previous studies have utilized genetic programming (GP) to derive correlations tailored to specific oil/brine systems, indicating that a lower initial IFT corresponds to a more stable emulsion with smaller water droplet size [43, 55].

Moreover, the introduction of rock particles (calcite/quartz) into emulsions increases water droplet size consistently across all cases. This effect has complex mechanisms: the dissolution of calcite/quartz in various brines raises pH, promoting more asphaltene adsorption at the water/oil interface, thereby reducing IFT and water droplet size. However, zeta-potential measurements reveal that both calcite and quartz particles exhibit negatively charged surfaces at low salinities, leading to repulsion between the oil phase and rock. At high salinities, rock particles become

positively charged, enhancing their adsorption at the water/oil interface and forming Pickering emulsions with increased stability and smaller droplet sizes. Additionally, Table 3 highlights an inverse relationship between the number and mean size of water droplets.

4. Conclusions

In this study, the primary objective was to investigate the impact of various rock types on asphaltene and emulsion stability (precipitation) in emulsified systems, particularly relevant to low-salinity waterflooding and potential formation damage in field applications. To accomplish this, we introduced calcite and quartz particles into different brines (DW, 10DSW, 2DSW, SW, and FW), generating a diverse range of emulsion samples with predetermined oil compositions. Additionally, we conducted supplementary tests, including UV-Vis absorbance analysis, interfacial tension (IFT) measurements, Fourier-transform infrared spectroscopy (FTIR), zeta-potential assessments, and image processing, to comprehensively understand our findings.

Based on the results, the following conclusions are made:

- In various emulsified systems prepared with crude oil and different brines, with and without the presence of rocks, there is observed migration of asphaltenes from the bulk of the oil to accumulate at the interface between water and oil. This phenomenon results in a reduction in UV-Vis absorbance in aged oil compared to fresh oil. Specifically, the UV-Vis absorbance decreases from 13.6 to 11, 10.5, and 10.5 for the 2DSW/oil, calcite/SW/oil, and quartz/2DSW/oil emulsions, respectively. Moreover, the presence of calcite/quartz particles in all brines amplifies the reduction in UV-Vis absorbance for oil. Calcite demonstrates a more

significant impact at lower salinities and a minor effect at higher salinities compared to quartz.

- The size of water droplets in emulsions, reflecting the presence of surfactant agents such as asphaltene at the water/oil interface, remains consistent after 1 and 24 hours. This suggests that no further asphaltene accumulates at the interface or deposits on the rock surface beyond the initial 1-hour period.
- The dissolution of calcite and quartz particles in different water types leads to an increase in pH, with the most significant increase observed in distilled water (DW). Quartz dissolution causes a critical pH change compared to calcite dissolution, except for 10 times diluted seawater (10DSW). In seawater (SW), both calcite and quartz dissolution results in a minor decrease in pH. Importantly, increased pH leads to greater asphaltene presence at the water/oil interface, particularly noticeable with calcite dissolution compared to quartz.
- At low salinities, both calcite and quartz particles repel asphaltenes due to their negative surface charge, leading to no adsorption onto the rock surface. However, at high salinities, calcite and quartz particles become positively charged, attracting unstable asphaltenes. This results in more asphaltene removal from the oil towards the particles' surface, particularly with calcite, showing 38% higher asphaltene deposition compared to quartz. The separation increases uniformly with rising water salinity.
- The presence of calcite and quartz particles increases water droplet size in emulsions, especially noticeable at lower salinities. At higher salinities, adhesion between asphaltenes and particles causes them to accumulate at the water/oil interface, forming Pickering emulsions, leading to smaller droplet sizes and more stable emulsions. This effect is more significant with calcite than quartz. Notably, the smallest droplet size occurs in SW/oil

emulsion in all cases, measuring 27.1, 36.1, and 33.6 without rock presence, with calcite, and with quartz, respectively.

In summary, our research sheds light on the complex relationship between brine types, rock presence, and salinity in asphaltene stability and emulsion properties relevant to petroleum engineering. To build on this, it is suggested to conduct similar studies using core material and under flow conditions for further investigation.

Supplementary Material

Additional detailed information, including A) XRD spectra of sandstone sample, B) microscopic images of water/oil emulsions in different brines, are provided in a separate document labeled "Supplementary Material."

Supplementary Material is available at:

[file:///C:/Users/SHAMILA/Downloads/Supplementary%20Material\(2\).pdf](file:///C:/Users/SHAMILA/Downloads/Supplementary%20Material(2).pdf)

References

- [1] Badizad , M. H., Koleini, M. M., Hartkamp, R., et al. "How do ions contribute to brine-hydrophobic hydrocarbon interfaces? An in silico study," J Colloid Interface Sci, vol. 575, pp. 337–346, Sep. 2020, doi: 10.1016/j.jcis.2020.04.060.
- [2] Bartels, W.-B., Mahani, H., Berg,S., et al. "Literature review of low salinity waterflooding from a length and time scale perspective," Fuel, vol. 236, pp. 338–353, Jan. 2019, doi: 10.1016/j.fuel.2018.09.018.
- [3] Tetteh, J. T., Brady, P. V., and Barati Ghahfarokhi, R. "Review of low salinity waterflooding in carbonate rocks: Mechanisms, investigation techniques, and future directions," Adv Colloid Interface Sci, vol. 284, p. 102253, Oct. 2020, doi: 10.1016/j.cis.2020.102253.

- [4] Mohammadkhani, S., Anabaraonye, B. U., Afrough, A., et al. "Crude oil–brine–rock interactions in tight chalk reservoirs: An experimental study," *Energies (Basel)*, vol. 14, no. 17, p. 5360, Sep. 2021, doi: 10.3390/EN14175360/S1.
- [5] Mokhtari, R., Anabaraonye, B. U., Afrough, A., et al. "Experimental investigation of low salinity water-flooding in tight chalk oil reservoirs," *J Pet Sci Eng*, vol. 208, p. 109282, Jan. 2022, doi: 10.1016/j.petrol.2021.109282.
- [6] Jafarbeigi, E., Salimi, F., Kamari, E., et al. "Effects of modified graphene oxide (GO) nanofluid on wettability and IFT changes: Experimental study for EOR applications," *Pet Sci*, vol. 19, no. 4, pp. 1779–1792, Aug. 2022, doi: 10.1016/J.PETSCI.2021.12.022.
- [7] An, S., Zhan, Y., Mahani, H., et al. "Kinetics of wettability alteration and droplet detachment from a solid surface by low-salinity: A lattice-Boltzmann method," *Fuel*, vol. 329, p. 125294, Dec. 2022, doi: 10.1016/J.FUEL.2022.125294.
- [8] Mogharrab, J. M., Ayatollahi, S., and Pishvaie, M. R. "Experimental study and surface complexation modeling of non-monotonic wettability behavior due to change in brine salinity/composition: Insight into anhydrite impurity in carbonates," *J Mol Liq*, vol. 365, p. 120117, Nov. 2022, doi: 10.1016/j.molliq.2022.120117.
- [9] Ghasemian, J., Riahi, S., Ayatollahi, S., et al. "Effect of salinity and ion type on formation damage due to inorganic scale deposition and introducing optimum salinity," *J Pet Sci Eng*, vol. 177, pp. 270–281, Jun. 2019, doi: 10.1016/J.PETROL.2019.02.019.
- [10] Moradi, M., Kazempour, M., French, J. T., et al. "Dynamic flow response of crude oil-in-water emulsion during flow through porous media," *Fuel*, vol. 135, pp. 38–45, Nov. 2014, doi: 10.1016/j.fuel.2014.06.025.
- [11] Rezaei, N. and Firoozabadi, A. "Macro- and microscale waterflooding performances of crudes which form w/o emulsions upon mixing with brines," *Energy and Fuels*, vol. 28, no. 3, pp. 2092–2103, Mar. 2014, doi: 10.1021/EF402223D.
- [12] Ali, M. A. and Islam, M. R. "The effect of asphaltene precipitation on carbonate-rock permeability: An experimental and numerical approach," *SPE Production & Facilities*, vol. 13, no. 03, pp. 178–183, Aug. 1998, doi: 10.2118/50963-PA.
- [13] Jafari Behbahani, T., Ghotbi, C., Taghikhani, V., et al. "Asphaltene deposition under dynamic conditions in porous media: Theoretical and experimental investigation," *Energy and Fuels*, vol. 27, no. 2, pp. 622–639, Feb. 2013, doi: 10.1021/EF3017255.
- [14] Ashoori, S. and Balavi, A. "An investigation of asphaltene precipitation during natural production and the CO₂ injection process," <http://dx.doi.org/10.1080/10916466.2011.633590>, vol. 32, no. 11, pp. 1283–1290, Jun. 2014, doi: 10.1080/10916466.2011.633590.
- [15] Kordestany, A., Hassanzadeh, H., and Abedi, J. "An experimental approach to investigating permeability reduction caused by solvent-induced asphaltene deposition in porous media,"

Canadian Journal of Chemical Engineering, vol. 97, no. 1, pp. 361–371, Jan. 2019, doi: 10.1002/CJCE.23238.

- [16] Mansouri, M., Ahmadi, Y., and Jafarbeigi, E. “Introducing a new method of using nanocomposites for preventing asphaltene aggregation during real static and dynamic natural depletion tests,” *Energy Sources, Part A: Recovery, Utilization and Environmental Effects*, vol. 44, no. 3, pp. 7499–7513, 2022, doi: 10.1080/15567036.2022.2113937.
- [17] Tavakkoli, M., Grimes, M. R., Liu, X., et al. “Indirect method: A novel technique for experimental determination of asphaltene precipitation,” *Energy & Fuels*, vol. 29, no. 5, pp. 2890–2900, May 2015, doi: 10.1021/ef502188u.
- [18] Shojaati, F., Mousavi, S. H., Riazi, M., et al. “Investigating the effect of salinity on the behavior of asphaltene precipitation in the presence of emulsified water,” *Ind Eng Chem Res*, vol. 56, no. 48, pp. 14362–14368, Dec. 2017, doi: 10.1021/ACS.IECR.7B03331/SUPPL_FILE/IE7B03331_SI_001.PDF.
- [19] Yarranton, H. W., Hussein, H., and Masliyah, J. H. “Water-in-hydrocarbon emulsions stabilized by asphaltenes at low concentrations,” *J Colloid Interface Sci*, vol. 228, no. 1, pp. 52–63, Aug. 2000, doi: 10.1006/jcis.2000.6938.
- [20] Mokhtari, R. and Ayatollahi, S. “Dissociation of polar oil components in low salinity water and its impact on crude oil–brine interfacial interactions and physical properties,” *Pet Sci*, vol. 16, no. 2, pp. 328–343, Apr. 2019, doi: 10.1007/s12182-018-0275-5.
- [21] Farhadi, H., Ayatollahi, S., and Fatemi, M. “The effect of brine salinity and oil components on dynamic IFT behavior of oil-brine during low salinity water flooding: Diffusion coefficient, EDL establishment time, and IFT reduction rate,” *J Pet Sci Eng*, vol. 196, p. 107862, Jan. 2021, doi: 10.1016/j.petrol.2020.107862.
- [22] Farhadi, H., Fatemi, M., and Ayatollahi, S. “Experimental investigation on the dominating fluid-fluid and rock-fluid interactions during low salinity water flooding in water-wet and oil-wet calcites,” *J Pet Sci Eng*, vol. 204, p. 108697, Sep. 2021, doi: 10.1016/j.petrol.2021.108697.
- [23] Tharanivasan, A. K., Yarranton, H. W., and Taylor, S. D. “Asphaltene precipitation from crude oils in the presence of emulsified water,” *Energy & Fuels*, vol. 26, no. 11, pp. 6869–6875, Nov. 2012, doi: 10.1021/ef301200v.
- [24] Tavakkoli, M., Panuganti, S. R., Taghikhani, V., et al. “Understanding the polydisperse behavior of asphaltenes during precipitation,” *Fuel*, vol. 117, pp. 206–217, Jan. 2014, doi: 10.1016/j.fuel.2013.09.069.
- [25] Farooq, U., Sjöblom, J., and Øye, G. “Desorption of asphaltenes from silica-coated quartz crystal surfaces in low saline aqueous solutions,” *J Dispers Sci Technol*, vol. 32, no. 10, pp. 1388–1395, Oct. 2011, doi: 10.1080/01932691.2010.505118.

- [26] Liu, F., Yang, H., Chen, T., et al. "Direct evidence of salinity and pH effects on the interfacial interactions of asphaltene-brine-silica systems." *Molecules* 25, no. 5 (2020): 1214, doi: 10.3390/molecules25051214
- [27] Hu, C., Sabio, J. C., Yen, A., et al. "Role of water on the precipitation and deposition of asphaltenes in packed-bed microreactors," *Ind Eng Chem Res*, vol. 54, no. 16, pp. 4103–4112, Apr. 2015, doi: 10.1021/IE5038775.
- [28] Joonaki, E., Erfani Gahrooei, H. R., and Ghanaatian, S. "Experimental study on adsorption and wettability alteration aspects of a new chemical using for enhanced oil recovery in carbonate oil reservoirs," *Journal of Unconventional Oil and Gas Resources*, vol. 15, pp. 11–21, Sep. 2016, doi: 10.1016/j.juogr.2016.05.001.
- [29] Lashkarbolooki, M., Riazi, M., Hajibagheri, F., et al. "Low salinity injection into asphaltenic-carbonate oil reservoir, mechanistical study," *J Mol Liq*, vol. 216, pp. 377–386, Apr. 2016, doi: 10.1016/j.molliq.2016.01.051.
- [30] Diar-Bakerly, B., Hirsemann, D., Kalo, et al. "Modification of kaolinite by Grafting of siderophilic ligands to the external octahedral surface," *Appl Clay Sci*, vol. 90, pp. 67–72, Mar. 2014, doi: 10.1016/j.clay.2013.12.020.
- [31] Liang, S., Li, C., Dai, L., et al. "Selective modification of kaolinite with vinyltrimethoxysilane for stabilization of Pickering emulsions." *Applied Clay Science* 161 (2018): 282-289, doi: 10.1016/j.clay.2018.04.038
- [32] Tambe, D. E. and Sharma, M. M. "The effect of colloidal particles on fluid-fluid interfacial properties and emulsion stability," *Adv Colloid Interface Sci*, vol. 52, pp. 1–63, Sep. 1994, doi: 10.1016/0001-8686(94)80039-1.
- [33] Xin-heng, C., and Tian, S. B. "Review and comprehensive analysis of composition and origin of high acidity crude oils." *China Petroleum Processing & Petrochemical Technology* 13, no. 1 (2011): 6, doi: 10.1021/am4053267
- [34] Monjezi, R., Ghotbi, C., Jafari Behbahani, T., et al. "Experimental investigation of dynamic asphaltene adsorption on calcite packs: The impact of single and mixed- salt brine films," *Can J Chem Eng*, vol. 97, no. 7, pp. 2028–2038, Jul. 2019, doi: 10.1002/cjce.23441.
- [35] Saraji, S., Goual, L., and Piri, M. "Dynamic adsorption of asphaltenes on quartz and calcite packs in the presence of brine films," *Colloids Surf A Physicochem Eng Asp*, vol. 434, pp. 260–267, Oct. 2013, doi: 10.1016/j.colsurfa.2013.05.070.
- [36] Nakatuka, Y., Yoshida, H., Fukui, K., et al. "The effect of particle size distribution on effective zeta-potential by use of the sedimentation method," *Advanced Powder Technology*, vol. 26, no. 2, pp. 650–656, Mar. 2015, doi: 10.1016/j.apt.2015.01.017.
- [37] Derkach, S. R. "Rheology of emulsions," *Adv Colloid Interface Sci*, vol. 151, no. 1–2, pp. 1–23, Oct. 2009, doi: 10.1016/j.cis.2009.07.001.

- [38] McClements, D. J. "Principles of ultrasonic droplet size determination in emulsions," *Langmuir*, vol. 12, no. 14, pp. 3454–3461, Jan. 1996, doi: 10.1021/la960083q.
- [39] Balavi, A., Ayatollahi, S., and Mahani, H. "The simultaneous effect of brine salinity and dispersed carbonate particles on asphaltene and emulsion stability," *Energy & Fuels*, vol. 37, no. 8, pp. 5827–5840, Apr. 2023, doi: 10.1021/acs.energyfuels.3c00293.
- [40] "IP 143/84, 1989 'Standard methods for analysis and testing of petroleum and related products'."
- [41] Mahani, H., Keya, A. L., Berg, S., et al. "Insights into the mechanism of wettability alteration by low-salinity flooding (LSF) in carbonates," *Energy and Fuels*, vol. 29, no. 3, pp. 1352–1367, Mar. 2015, doi: 10.1021/EF5023847.
- [42] Taherian, Z., Saeedi Dehaghani, A., Ayatollahi, S., et al. "The mechanistic investigation on the effect of the crude oil /brine interaction on the interface properties: A study on asphaltene structure," *J Mol Liq*, vol. 360, p. 119495, Aug. 2022, doi: 10.1016/j.molliq.2022.119495.
- [43] Ameri, A., Esmailzadeh, F., and Mowla, D. "Effect of low-salinity water on asphaltene precipitation," *J Dispers Sci Technol*, vol. 39, no. 7, pp. 1031–1039, Jul. 2018, doi: 10.1080/01932691.2017.1381616.
- [44] Moeini, F., Hemmati-Sarapardeh, A., Ghazanfari, M.H., et al. "Toward mechanistic understanding of heavy crude oil/brine interfacial tension: The roles of salinity, temperature and pressure," *Fluid Phase Equilib*, vol. 375, pp. 191–200, Aug. 2014, doi: 10.1016/j.fluid.2014.04.017.
- [45] Ayirala, S. C., Al-Saleh, S. H., and Al-Yousef, A. A. "Microscopic scale interactions of water ions at crude oil/water interface and their impact on oil mobilization in advanced water flooding," *J Pet Sci Eng*, vol. 163, pp. 640–649, Apr. 2018, doi: 10.1016/j.petrol.2017.09.054.
- [46] Mahmoudvand, M., Javadi, A., and Pourafshary, P. "Brine ions impacts on water-oil dynamic interfacial properties considering asphaltene and maltene constituents," *Colloids Surf A Physicochem Eng Asp*, vol. 579, p. 123665, Oct. 2019, doi: 10.1016/j.colsurfa.2019.123665.
- [47] Shahsavani, B., Riazi, M., and Malayeri, M. R. "Asphaltene instability in the presence of emulsified aqueous phase," *Fuel*, vol. 305, p. 121528, Dec. 2021, doi: 10.1016/j.fuel.2021.121528.
- [48] Demir, A. B., Bilgesu, H. I., and Hascakir, B. "The effect of clay and salinity on asphaltene stability," in *All Days*, SPE, May 2016. doi: 10.2118/180425-MS.
- [49] Mahani, H., Keya, A. L., Berg, S., et al. "Electrokinetics of carbonate/brine interface in low-salinity waterflooding: Effect of brine salinity, composition, rock type, and pH on ζ Potential and a surface-complexation model," *SPE Journal*, vol. 22, no. 01, pp. 53–68, Feb. 2017, doi: 10.2118/181745-PA.

- [50] Rahbar, M., Roosta, A., Ayatollahi, S., et al. "Prediction of three-dimensional (3-D) adhesion maps, using the stability of the thin wetting film during the wettability alteration process," *Energy & Fuels*, vol. 26, no. 4, pp. 2182–2190, Apr. 2012, doi: 10.1021/ef202017a.
- [51] Joonaki, E., Hassanpour Youzband, A., Burgass, R., et al. "Effect of water chemistry on asphaltene stabilised water in oil emulsions - a new search for low salinity water injection mechanism," 79th EAGE Conference and Exhibition 2017, vol. 2017, no. 1, pp. 1–5, Jun. 2017, doi: 10.3997/2214-4609.201701297/CITE/REFWORKS.
- [52] Zaker, S., Parvizi, R., Ghaseminejad, E., et al. "Effect of brine type and pH on the interfacial tension behavior of carbonated brine/crude oil," *J Dispers Sci Technol*, vol. 42, no. 8, pp. 1184–1195, Jun. 2021, doi: 10.1080/01932691.2020.1735409.
- [53] Buenrostro-Gonzalez, E., Groenzin, H., Lira-Galeana, C., et al. "The overriding chemical principles that define asphaltenes," *Energy and Fuels*, vol. 15, no. 4, pp. 972–978, Jul. 2001, doi: 10.1021/EF0100449.
- [54] Ridwan, M. G., Kamil, M. I., Sanmurjana, M., et al. "Low salinity waterflooding: surface roughening and pore size alteration implications. " *Journal of Petroleum Science and Engineering* 195 (2020): 107868, doi: 10.1016/j.petrol.2020.107868
- [55] Kazemzadeh, Y., Ismail, I., Rezvani, H., et al. "Experimental investigation of stability of water in oil emulsions at reservoir conditions: Effect of ion type, ion concentration, and system pressure," *Fuel*, vol. 243, pp. 15–27, May 2019, doi: 10.1016/j.fuel.2019.01.071.

Shahab Ayatollahi is the Director of Petroleum Engineering Group and a Professor at the Department of Chemical and Petroleum Engineering at Sharif University of Technology in Tehran. He received his BSc and MSc in Chemical Engineering both from Shiraz University and received his PhD in Chemical Engineering in 1995 from the University of Waterloo, Canada. He has published more than three hundred papers related to oil reservoir engineering. The research works he is pioneering are focused on EOR from tight and asphaltenic reservoirs, pore structure, rock-fluid and fluid-fluid interactions, and multiphase flow in porous media.

Hassan Mahani is an Associate Professor of Petroleum Engineering at Sharif University of Technology. He holds a PhD degree in Petroleum Engineering from Imperial College London and a MSc degree in Chemical Engineering from Sharif University of Technology. Prior to joining Sharif University of Technology, he worked as principal investigator and scientist at Shell Technology Centers in The Netherlands. He currently serves as Associate Editor for SPE Journal and Geoenergy Science and Engineering Journal. His research is geared toward fundamental understanding, quantitative evaluation, modeling and prediction of multi-phase flow in porous media with application to IOR/EOR, geo-engineering and environment. His current activities focus on water-based/low-salinity EOR; Underground Hydrogen & Energy Storage, Contaminant Gas Storage; Pore-scale physics & Digital rocks; Geochemistry and Geomechanics.

Amir Hossein Salari is a graduate of petroleum engineering from Sharif University of Technology and currently employed in the oil, gas, and petrochemical industry at Petro Artan Part Company. He obtained his bachelor's and master's degrees in petroleum engineering, specializing in hydrocarbon reservoirs, in 2009 from Sahand University of Technology in Tabriz and in 2023 from Sharif University of Technology in Tehran, respectively. His expertise lies in enhancing oil extraction methods and studying the interaction between water and oil. Additionally, he has contributed articles to this field.

Ali Balavi is currently a PhD student (since 2019) at Sharif University of Technology. He received his bachelor's and master's degrees in Drilling Engineering, in 2009, and Production Engineering, in 2011, from Petroleum University of Technology (PUT). He has been working at National Iranian Oil Company (NIOC) since 2010 and currently (since 2018) is working as production engineering project supervisor in Karoon Company. He managed to publish articles on the stability and deposition of asphaltene during gas and water injection operations in southwestern Iran reservoirs and has a history of cooperation in several research-industrial projects. His research interests include enhanced oil recovery from oil reservoirs and asphaltene stability.

Figure captions

Figure 1. The schematic of the indirect method to investigate asphaltene stability in water in oil emulsified systems containing solid particles

Figure 2. UV-Vis absorbance of fresh/aged oil phase for different emulsion systems

Figure 3. The equilibrium pH change for calcite or quartz suspensions in different aqueous phases (Formation Water (FW), Sea Water (SW), 2 and 10 times diluted SW (2DSW, 10DSW), Distillated Water (DW))

Figure 4. The rock/brine zeta-potential for different rock/brines (Formation Water (FW), Sea Water (SW), 2 and 10 times diluted SW (2DSW, 10DSW), Distillated Water (DW)) at equilibrium pH

Figure 5. The FTIR absorbance of the fresh crude oil

Figure 6. The amount of adsorbed asphaltene onto rock surface for different cases

Figure 7. Initial IFT between fresh oil and different brines (Formation Water (FW), Sea Water (SW), 2 and 10 times diluted SW (2DSW, 10DSW), Distillated Water (DW)) containing particles

Figure 8. Final IFT between aged oil and different brines (Formation Water (FW), Sea Water (SW), 2 and 10 times diluted SW (2DSW, 10DSW), Distillated Water (DW)) containing particles

Figure 9. The change of UV-Vis absorbance and IFT change for different experiments

Figure 10. The mean size of water droplets in different emulsified systems after 1 hour of mixing

Figure 11. The mean size of water droplets in different emulsified systems after 24 hours of mixing

Figure S.1. Microscopic images of water-in-oil emulsions after 1 and 24 hours of mixing/stirring for “no-rock” experiments

Figure S.2. Microscopic images of water-in-oil emulsions after 1 and 24 hours of mixing/stirring for “dissolved calcite rock” experiments

Figure S.3. Microscopic images of water-in-oil emulsions after 1 and 24 hours of mixing/stirring for “solid calcite” experiments

Figure S.4. Microscopic images of water-in-oil emulsions after 1 and 24 hours of mixing/stirring for “dissolved sandstone rock” experiments

Figure S.5. Microscopic images of water-in-oil emulsions after 1 and 24 hours of mixing/stirring for “Solid sandstone” experiments

Figure S.6. Microscopic images of 10DSW/oil emulsions after 1 hour in the first group of experiments

Figure S.7. Gray microscopic images of 10DSW/oil emulsions after 1 hour in the first group of experiments

Figure S.8. Mineral composition of the sandstone sample from X-ray diffraction (XRD) analysis

Table captions

Table 1. The physical properties (at ambient conditions) and SARA fraction of the used crude oil

Table 2. The salt concentrations used in different brines (Formation Water (FW), Sea Water (SW), 2 and 10 times diluted SW (2DSW, 10DSW), Distillated Water (DW))

Table 3. Total detected water droplets number in the microscopic images of different emulsified systems

Figures

Figure 1.

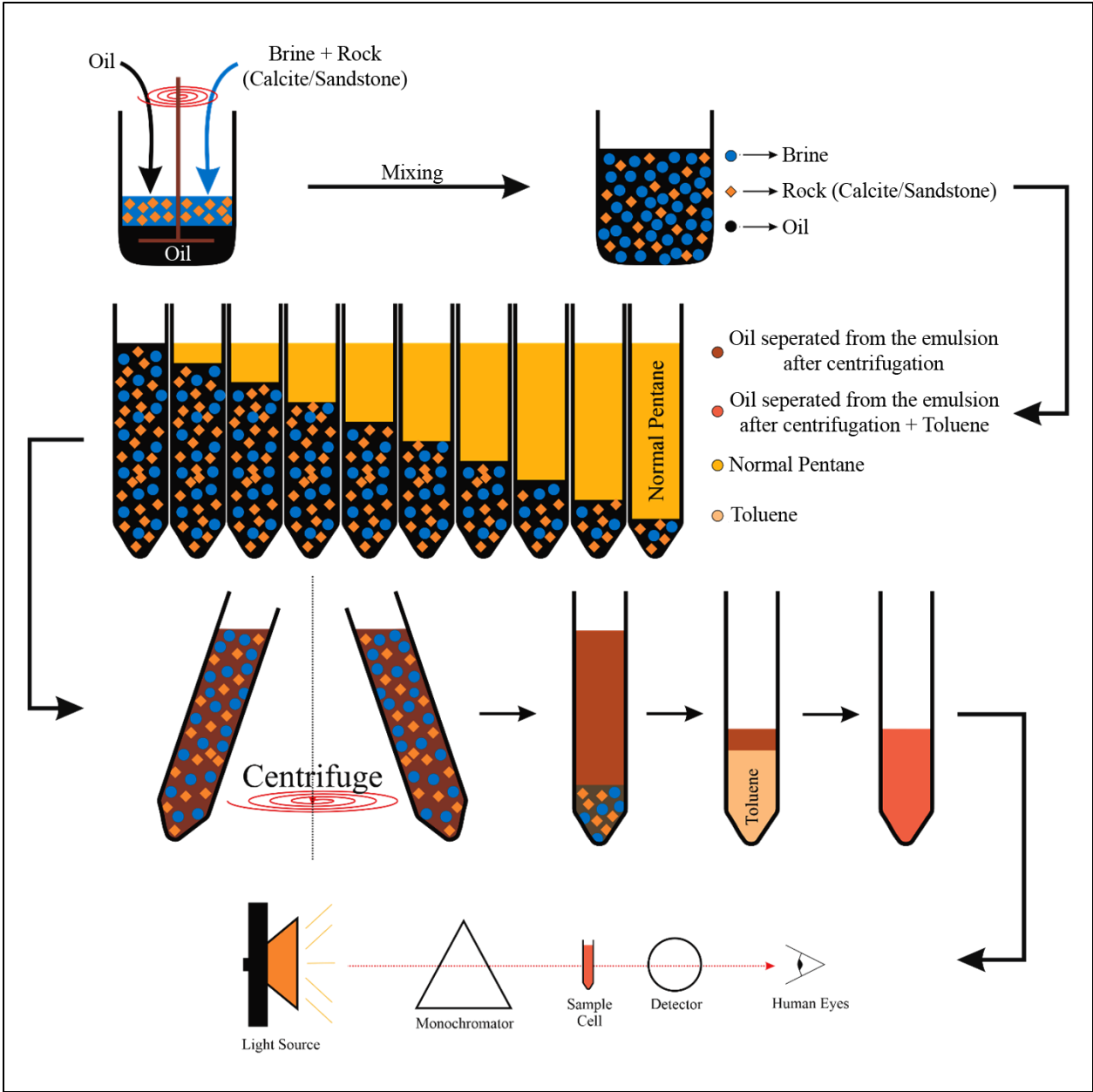


Figure 2.

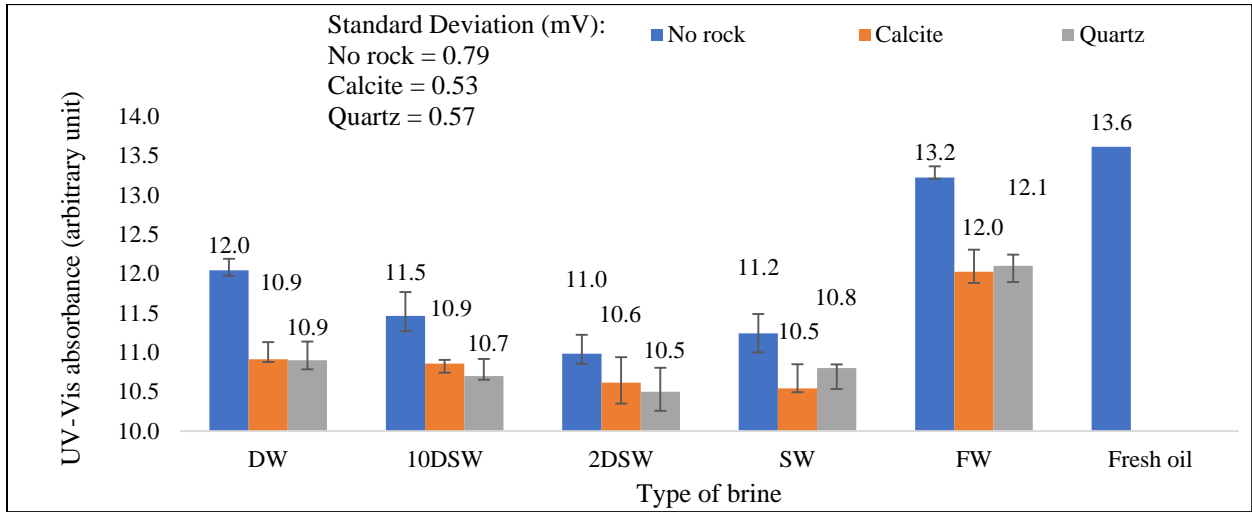


Figure 3.

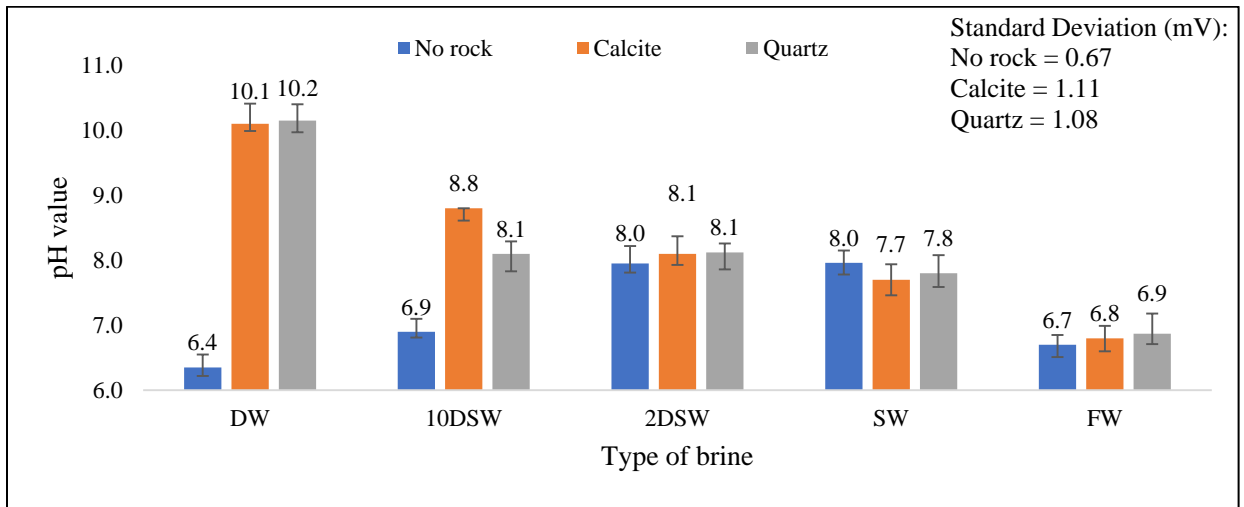


Figure 4.

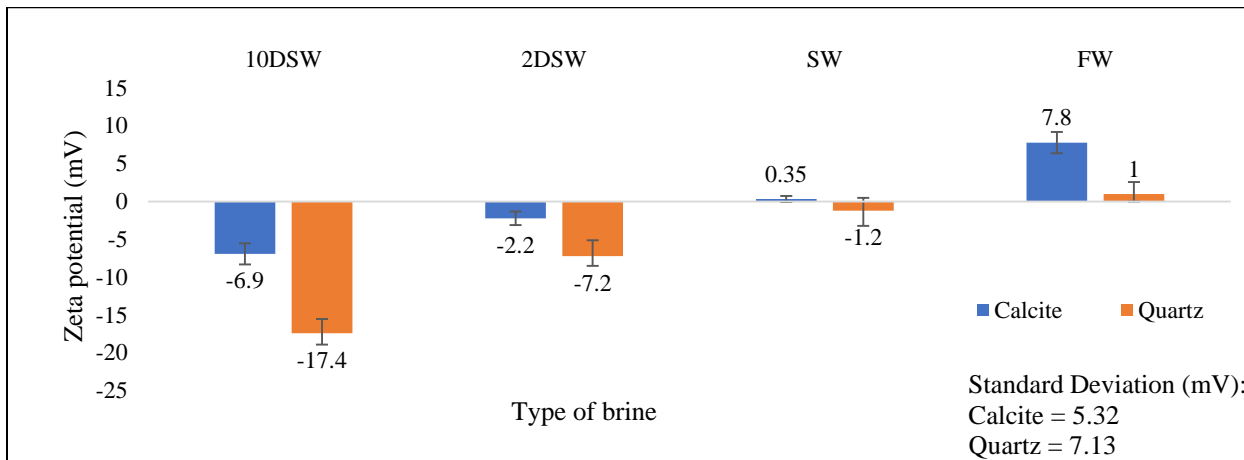


Figure 5.

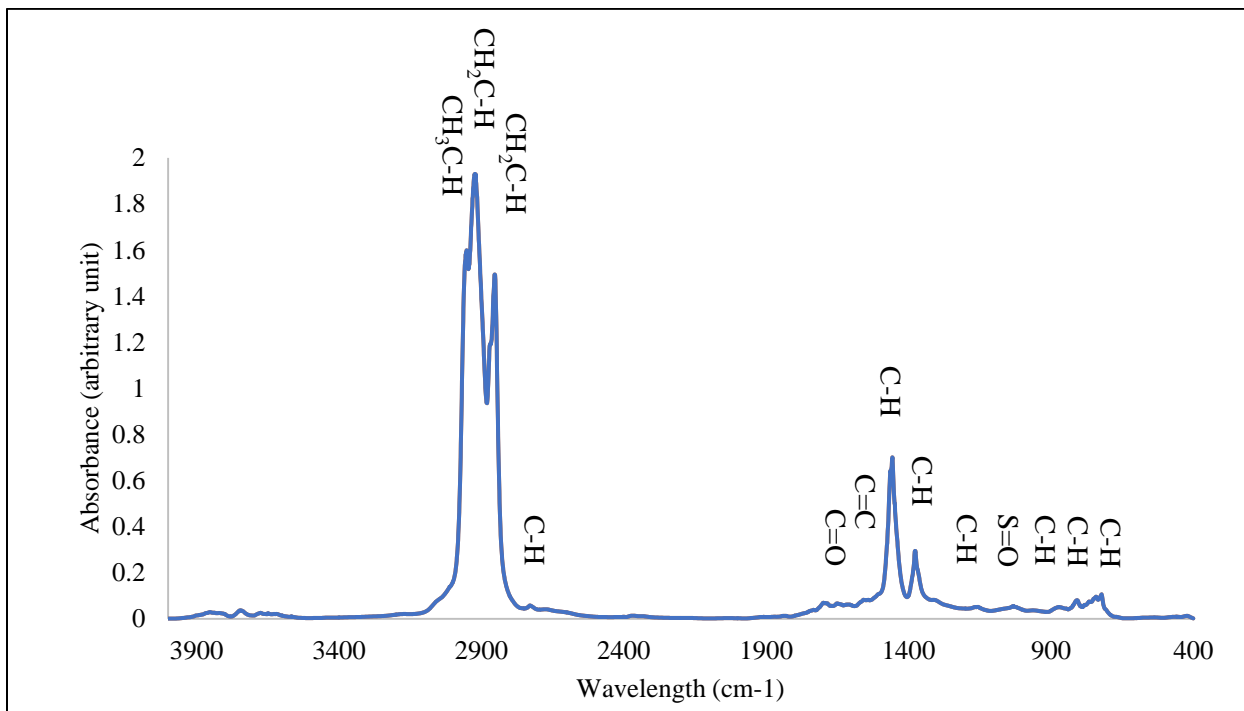


Figure 6.

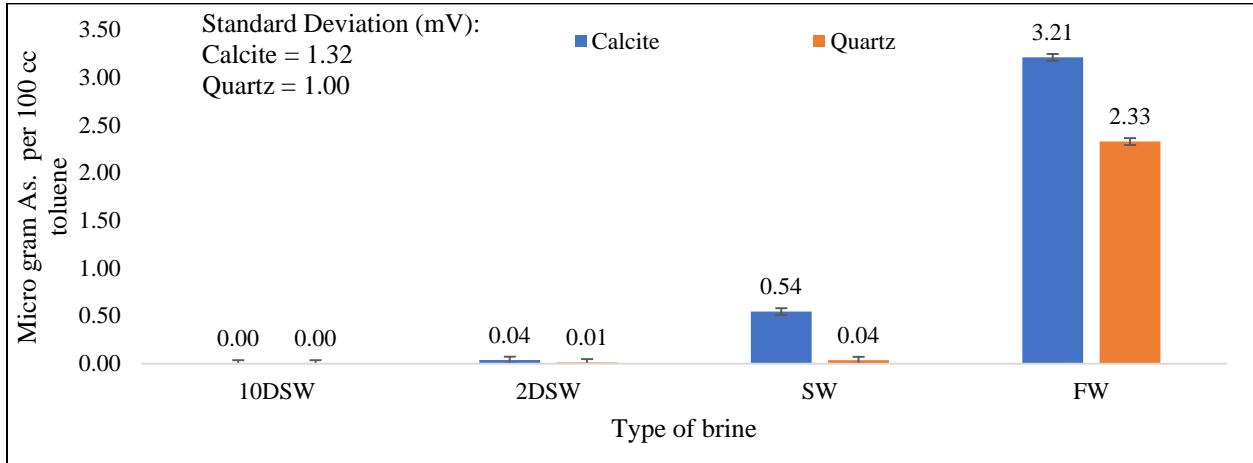


Figure 7.

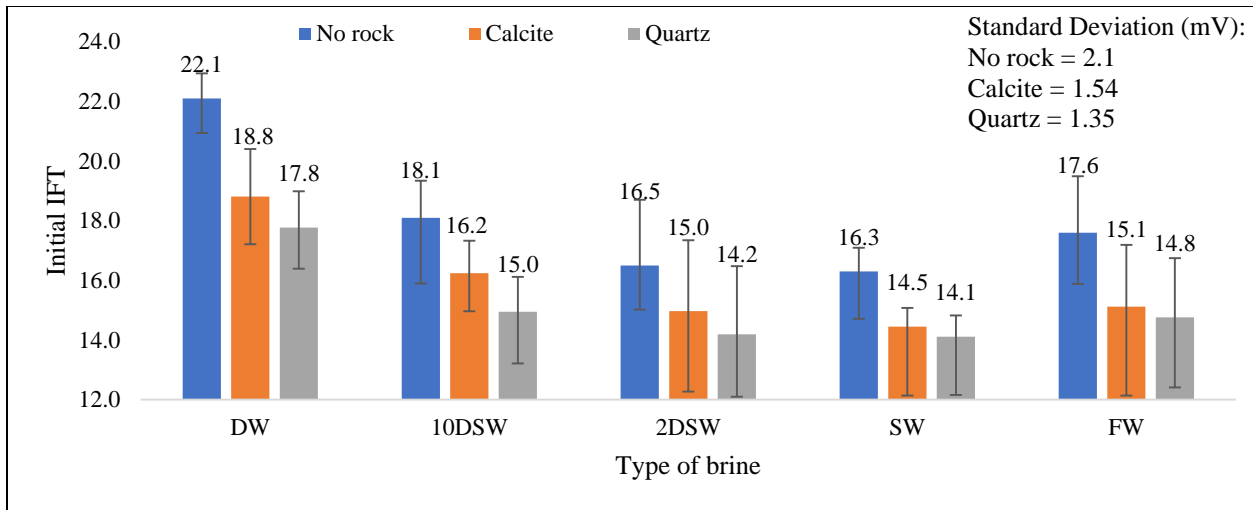


Figure 8.

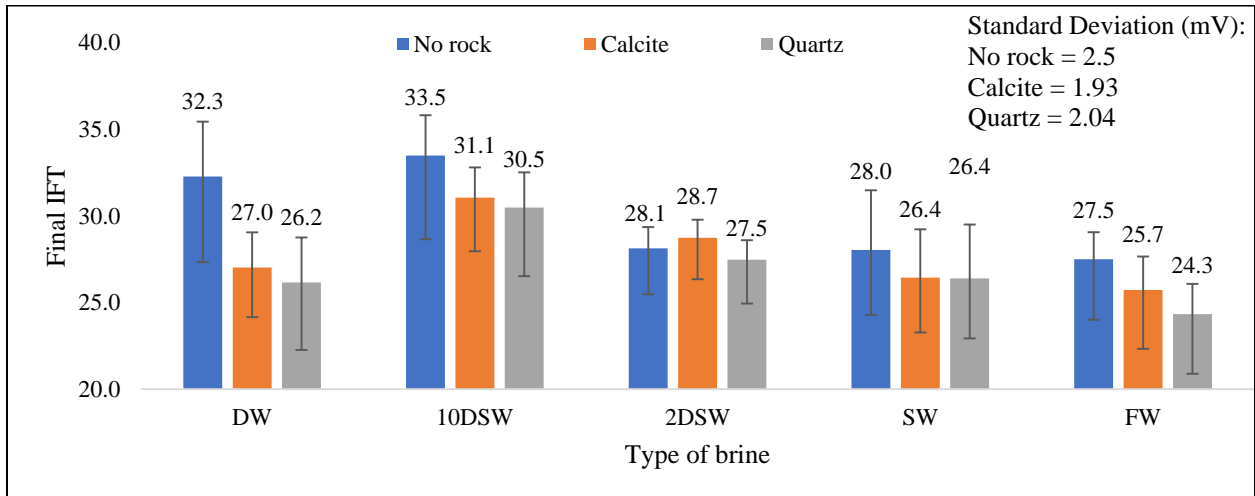


Figure 9.

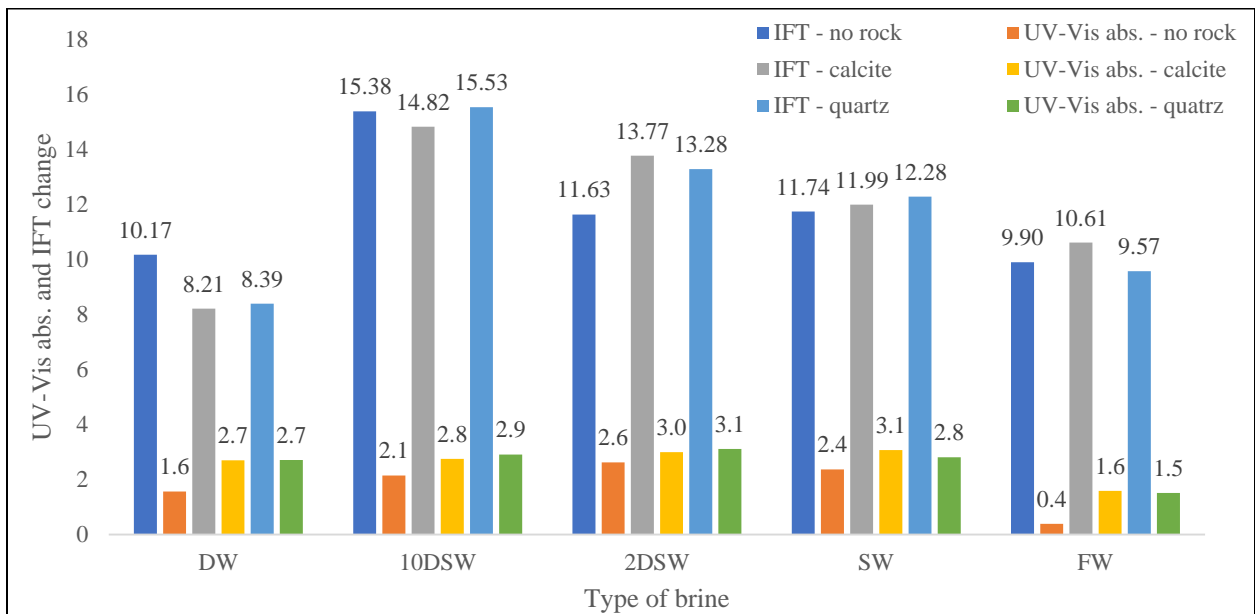


Figure 10.

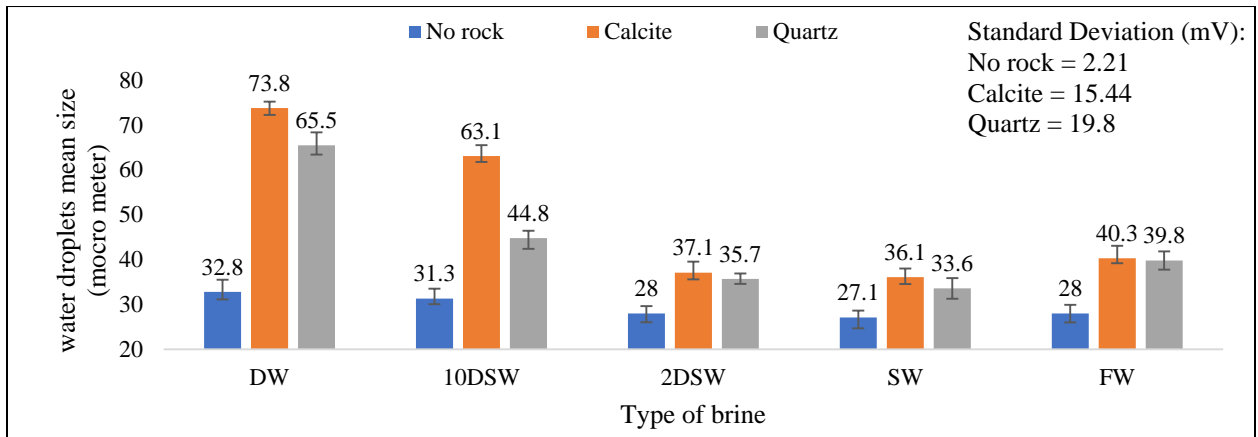
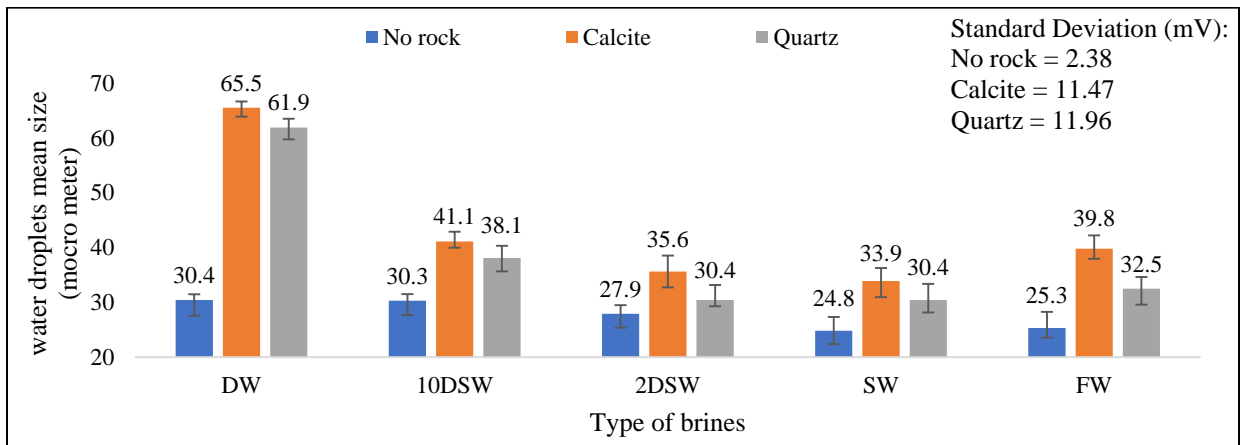


Figure 11.



Tables

Table 1.

Asphaltenes (wt%)	1.5
Resins (wt%)	7.5
Aromatics (wt%)	20.5
Saturates (wt%)	70.5
Total acid number (mg KOH/g oil)	0.11
Density (g/cc) @ 25 °C	0.84
Viscosity (cP) @ 25 °C	7.5

Table 2.

Salt type	FW	SW	2DSW	10DSW
NaCl (g/L)	154.031	25.576	12.788	2.558
KCl (g/L)	1.193	1.118	0.559	0.112
CaCl ₂ .2H ₂ O (g/L)	24.110	1.764	0.882	0.176
MgCl ₂ .6H ₂ O (g/L)	8.933	11.995	5.998	1.200
Na ₂ SO ₄ (g/L)	0.426	6.818	3.409	0.682
NaHCO ₃ (g/L)	0.672	0.336	0.168	0.034
pH	6.7	8.0	8.0	6.9
Total Dissolved Solids (ppm)	189365	47607	23804	4761
Ionic Strength (mol/L)	3.29	0.81	0.41	0.08

Table 3.

Emulsified system	Brine Type	Total detected water droplets in an area of 20 mm x 20 mm of a microscope slide	
		After 1 hour	After 24 hours
No rock	DW	5998	6398
	10DSW	6239	6419
	2DSW	6749	6851
	SW	7064	7645
	FW	6752	7416
With calcite	DW	2814	3305
	10DSW	3599	5087
	2DSW	5516	5614
	SW	5547	5842
	FW	5194	5278
With quartz	DW	1297	1264
	10DSW	2223	2553
	2DSW	1091	1529
	SW	2034	1534
	FW	1162	1976

